

低叶尖马赫数开式叶轮气动声源数值研究

万剑峰

(上海理工大学 能源与动力工程学院, 上海 200093)

摘要:采用大涡模拟结合 FW-H 方程的混合方法对低叶尖马赫数开式叶轮流场和气动噪声进行全尺寸模拟, 并对此类开式叶轮气动声源特性进行研究。声压级在空间和频域上的分布表明: 此类开式叶轮声源包括叶片转动时产生的单极子声源、偶极子声源和叶片尾涡产生的四极子声源, 基本不存在桨涡干涉噪声, 尾涡四极子声源耗散快, 无法传输到叶轮下游, 在叶轮下游区域未见明显四极子声源; 单极子噪声占开式叶轮气动噪声的大部分, 偶极子噪声占重要部分, 偶极子声源主要集中在叶顶的前缘和尾缘区域, 前缘声压大于尾缘声压, 吸力面声压大于压力面声压。

关键词:开式叶轮; 气动噪声; 大涡模拟; FW-H 方程

中图分类号: TB533.1 文献标识码: A

DOI:10.16146/j.cnki.rndlgc.2015.04.013

引言

目前对风力机的全尺寸实验研究还存在着一定的难度, 由于风力机气动噪声发声机制不明确, 高效噪声抑制方法还有待研究, 数值模拟将成为风力机气动噪声研究的重要手段^[1]。文献[2]采用缩比模型实验研究 CLOR 叶型旋翼气动噪声, 并用雷诺时均法求解压力脉动, 再用 Kirchhoff 方法计算远场声场。文献[3]对单极小型散热风扇进行大涡(LES)模拟发现旋转噪声与实验测量值一致。文献[4]采用大涡模拟方法研究了风轮尾迹流动, 得到尾迹湍流脉动特性。文献[5]综述前人研究认为, 开式叶轮中的气动降噪设计难度较大, 技术不够成熟, 推测气动噪声可以通过控制涡流来控制噪声。文献[6]采用大涡模拟方法研究湍流的拟序结构, 认为大涡模拟比雷诺平均法能更好揭示流动细节和瞬态过程。文献[7]通过比较各种气动噪声计算方法, 认为采用大涡模拟和 FW-H 积分相结合更有优势。

目前, 对开式叶轮气动噪声在气动设计降噪方面并无有效降噪声措施, 需对开式叶轮气动噪声声

源特性进一步研究, 实验研究方法不成熟, 模拟研究主要集中在高叶尖马赫数旋翼和小型冷却风扇, 对较大尺寸低叶尖马赫数(<0.5)的开式叶轮流动和气动噪声缺乏全面的认识。

本研究采用大涡模拟结合 FW-H 方法模拟低叶尖马赫数下的全尺寸开式叶轮流场和气动声场, 得到开式叶轮流场结构和声源分布数据, 为采用合理降噪措施提供依据。

1 流动和声场的数值模拟方法

1.1 流动控制方程

为精确捕捉小尺度流动特征, 流动模拟采用大涡模拟的 Smagorinsky 亚格子模型进行计算, 其控制方程为^[8-9]:

$$\frac{\partial \rho}{\partial t} + \frac{\partial}{\partial x_i} (\rho u_i) = 0 \quad (1)$$

$$\frac{\partial}{\partial t} (\rho u_i) + \frac{\partial}{\partial x_j} (\rho u_i u_j) = (\mu(T) + \rho v_{sgs}) \cdot$$

$$\frac{\partial}{\partial x_j} \left(\frac{\partial u_i}{\partial x_j} + \frac{\partial u_j}{\partial x_i} - \frac{2}{3} \frac{\partial u_k}{\partial x_k} \delta_{ij} \right) - \frac{\partial p}{\partial x_i} \quad (2)$$

式中: u_i —过滤后的尺度速度分量; v_{sgs} —亚格子粘系数; δ_{ij} —克罗内克符号。

$$v_{sgs} = \{C_s \Delta [1 - \exp(-y^+ / a)]\}^2 \cdot \sqrt{2S_{ij}(u) S_{ij}(u)} \quad (3)$$

式中: S_{ij} —可解尺度的变形率张量; Δ —过滤尺度; C_s 、 a —模型常数, 在模拟中取 $C_s = 1.0$ 、 $a = 26$ 。

为了加快 LES(大涡模拟)的收敛速度, 以定常 RANS(雷诺平均模拟)计算收敛值作为大涡模拟的初场。当数值计算的结果呈现随时间周期性变化时, 则认为 LES 计算收敛。

1.2 声场控制方程

在远场线性化假设和控制面为固壁边界的条件

收稿日期: 2014-07-28; 修订日期: 2014-11-05

基金项目: 国家自然科学基金资助项目(51276116)

作者简介: 万剑峰(1977-), 男, 江西鹰潭人, 河南理工大学讲师。

下, FW-H 方程化简为:

$$\left(\frac{1}{c^2} \frac{\partial}{\partial t^2} - \frac{\partial^2}{\partial x_i^2} \right) p'(x_i, t) = \frac{\partial}{\partial t} [\rho_0 v_n] \delta(f) - \frac{\partial}{\partial x_i} [P'_{ij} n_j \delta(f)] + \frac{\partial}{\partial x_i x_j} [T_{ij} H(f)] \quad (4)$$

式中: c —当地声速; $p'(x_i, t)$ —观测点在 t 时刻的声压值; ρ, u_i, P_{ij} —密度、速度和应力张量; v_n —控制面法向速度; T_{ij} —赖特希尔张量; $f(X, t) = 0$ —封闭控制面函数; $H(f)$ —亥维赛德函数; 下标 0 表示未扰动量, 下标 n 表示在控制面外法向的方向, 上标 “ $'$ ” 表示扰动量。

$$T_{ij} = P'_{ij} + \rho u_i u_j - c^2 \rho \delta_{ij} \quad (5)$$

式(4) 等号右边为声源, 依次分别表示单极子声源、偶极子声源和四极子声源。在开式叶轮里单极子声源由叶片扫过后造成密度变化而产生, 偶极子声源由叶片表面与气流作用而产生, 四极子声源为体声源与涡流有关。

1.3 计算网格设计

开式叶轮叶片为克拉克-Y 叶型等值无扭叶片, 叶高 400 mm, 弦长 60 mm。叶轮采用两叶片中心对称布置, 安装角 5°, 图 1 表示开式叶轮计算域。计算域被分为 3 个区域, 来流静止区域、叶轮旋转区域和尾流静止区域, 每个区域的交界面类型设计为 interface(接口), Y 向总长为 $3d + 8d + 10d = 21d$ (d 为弦长), 叶轮布置在叶轮旋转区域 $Z=0$ 平面上内。

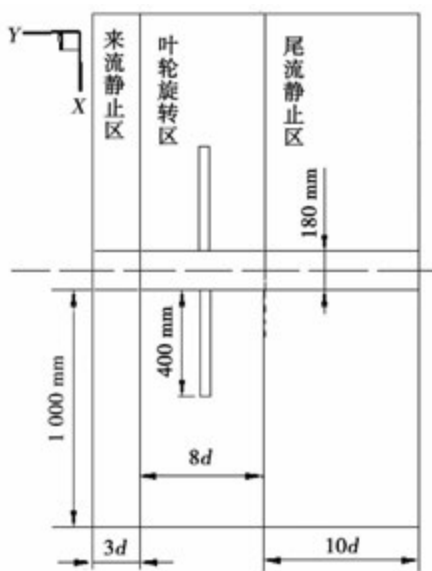


图 1 开式叶轮计算域(d 为弦长)

Fig. 1 Open rotor computational domain
(‘ d ’ is chord length)

图 2 表示网格划分结构, 总网格数 310 万, 叶片和轴面设为无滑移边界, 叶片和转动轴表面第一层网格高度设为 0.001 mm, 采用结构化网格。

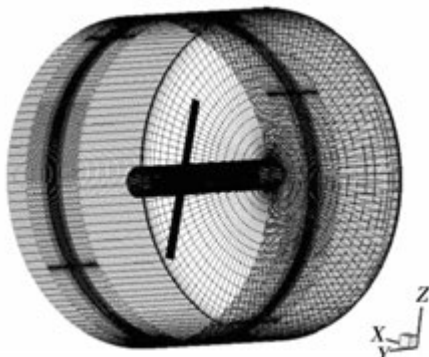


图 2 开式叶轮计算网格

Fig. 2 Open rotor computation grid

在求解开式叶轮计算过程中, 定常时采用多重参考系模型, 旋转轴为 Y 轴(Y 轴与叶轮轴中心一致), 来流静止区和尾流静止区运动形式设置为静止。在非定常计算时, 为了提高计算精度, 采用滑移网格处理方式, 随时间推进, 旋转区域的网格随着转动部件转动, 静止区域的网格则保持静止。

2 计算结果分析

计算工况为转速 30 r/s 匀速转动, 叶尖马赫数为 0.22。外边界设置为压力边界, 取值为 1 个大气压。

流场和声场计算采用 FLUENT V13.0 进行计算。定场的湍流计算模型采用 RNG $k-\epsilon$ 模型; 非定场采用大涡模型中的 Smagorinsky(亚格子) 模型, 双时间步法迭代求解, 时间步长 1×10^5 s, 每个时间步迭代 30 步。当数值计算的结果呈现随时间周期性变化时, 则认为 LES 计算收敛。采用有限体积法离散方程, 时间项离散采用二阶隐式格式, 对流项采用二阶迎风格式, 扩散项采用二阶中心差分格, 压力速度耦合迭代采用 Simple 算法。

图 3(a) 和图 3(b) 依次为叶片吸力面和压力面声功率级分布图, 叶片表面高声功率级主要集中在叶片前缘处叶顶区域, 表明表面声源幅值前缘强于尾缘, 叶顶强于叶根, 吸力面强于压力面, 表面声源幅值最强区域在叶顶处前缘区域。

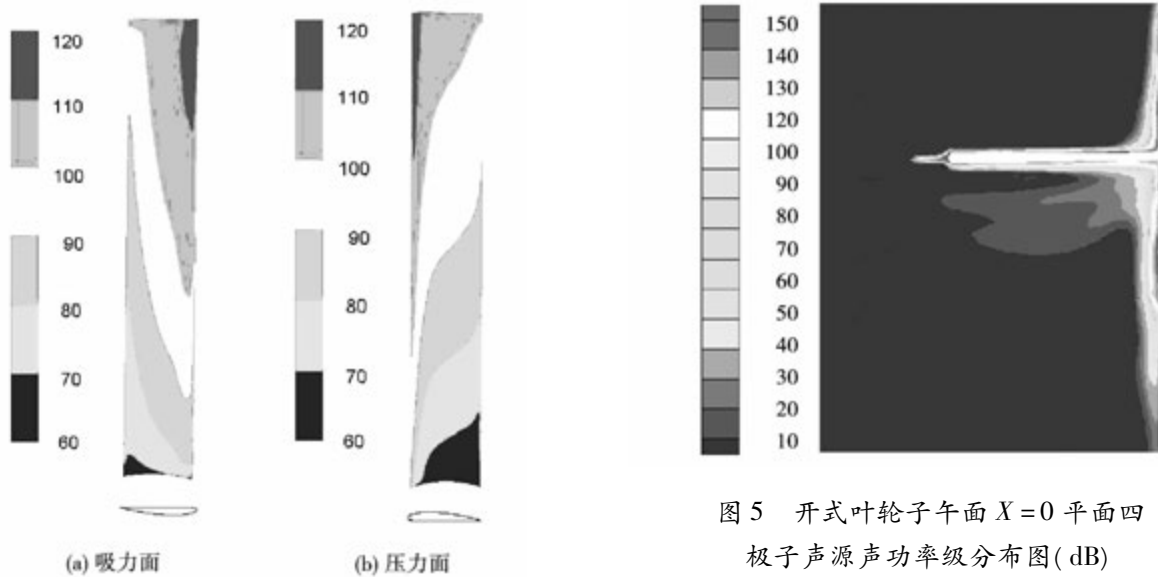


图 3 叶片表面声功率级(dB)

Fig. 3 Sound power level of blade surface(dB)

分析桨涡是否干涉,对开式叶轮的气动噪声研究有重要意义。图 4 为 300/s 的涡量等值面图,300/s 涡量值极低,叶片仍无法形成较长的涡量尾迹,表明上叶片的涡量尾迹与下叶片不会相交,故此类开式叶轮无明显桨涡干涉噪声。

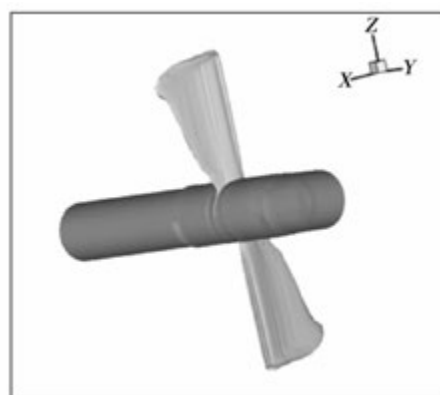


图 4 开式叶轮涡量为 300/s 时的等值面

Fig. 4 300/s open rotor vorticity isosurface

图 5 为开式叶轮 $X = 0$ 平面四极子声源声功率分布图。图中只有两条条形区域,且下一条要比上一条弱,表明仅在叶片尾涡区域产生较强的四极子声源,四极子声源只能持续旋转一周的时间,超过一周后,四极子声源迅速耗散,其无法通过流动方式传输到下游。

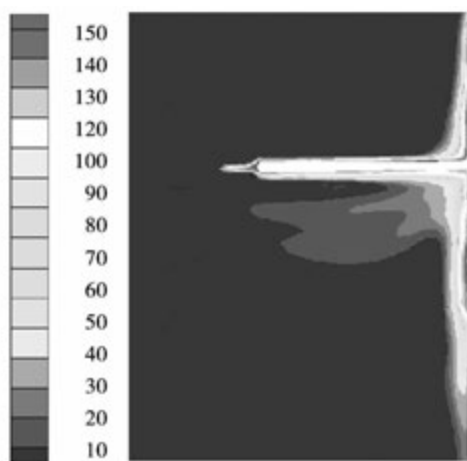
图 5 开式叶轮子午面 $X = 0$ 平面四极子声源声功率级分布图(dB)Fig. 5 open rotor meridian plane quadrupole source sound power level distribution ($X = 0$ plane) (dB)

图 6 表示开式叶轮单极子噪声声压频域分布,声压测点在开式叶轮风前与转动轴夹角 45°,距叶轮中心 1.5 m 处,图中出现了以叶轮通过频率(60 Hz)为间隔的尖峰,且越来越小。

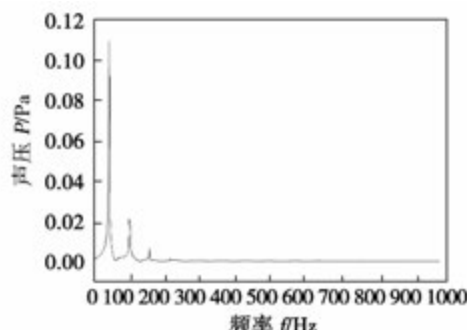
图 6 开式叶轮一测点单极子噪声声压频域分布
(测点: 转动轴夹角 45°、距叶轮中心 1.5 m 处)Fig. 6 Open rotor monopole noise sound pressure frequency distribution at a measuring point
(Measuring point: angle 45° from the rotation axis,
and 1.5 m from the center of the open rotor)

图 7 表示开式叶轮偶极子噪声声压频域分布,图中出现了有间隔的尖峰,测点同上,但是其间隔频率却不固定,在较高频率区域,出现小幅扰动。从图 6 和图 7 尖峰值的大小来看,偶极子要小于单极子,表明开式叶轮在叶尖低马赫数下,单极子噪声所含

成分要高于偶极子噪声,从高频的小扰动来看,偶极子噪声能产生少量的宽频噪声。

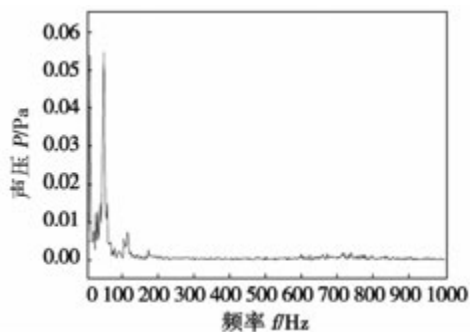


图 7 开式叶轮一测点偶极子噪声频域分布
(测点: 转动轴夹角 45°、距叶轮中心 1.5 m 处)

Fig. 7 Open rotor dipole noise frequency distribution at a measuring point

(Measuring point: angle 45° from the rotation axis, and 1.5 m from the center of the open rotor)

3 结 论

(1) 表面声源幅值最强处在叶顶前缘区域。涡量沿尾迹迅速耗散,无法维持到一个叶片通过周期,不存在明显桨涡干涉现象,无桨涡干涉噪声。

(2) 四极子声源仅由开式叶轮尾缘涡脱落产生,其耗散迅速,最多维持一个旋转周期,就几乎消失,不能对远场声压产生影响。

(3) 单极子声源占气动噪声主要部分,偶极子声源占重要部分。单极子噪声占开式叶轮气动噪声的大部分,它是以叶片通过频率为基频的离散信号,偶极子噪声是开式叶轮气动噪声的重要来源,它在低频区有离散信号,在高频区域有宽频信号,其主要分布在叶顶附近。

远场降噪重点应考虑对叶顶前缘进行优化,近场降噪需要加强叶片尾缘设计以降低尾流四极子声源强度。

参考文献:

- [1] 李晓东,许影博,江 曼.风力机气动噪声研究现状与发展趋势 [J].应用数学和力学,2013,34(10):1083–1090.
LI Xiao-dong, XU Ying-bo, JIANG Wen. Research status and trend of wind turbine aerodynamics noise [J]. Applied Mathematics and Mechanics, 2013, 34(10) : 1083 – 1090.
- [2] 军樊枫,赵国庆,徐国华.改进型 CLOR 桨尖旋翼悬停状态气动噪声特性试验与预估分析 [J].空气动力学学报,2013,31(4):454–461.
JUN Fan-feng, ZHAO Guo-qing, Xu Guo-hua. Investigations on acoustic characteristics of rotor with improved CLOR blade-tip in hover based on experimental and prediction method [J]. Aerodynamics Journal, 2013, 31(4) : 454 – 461.
- [3] 伍文华,杜平安,陈 燕,等.大涡模拟在轴流风扇气动噪声仿真中的应用 [J].机械设计与制造,2013(1):63–65.
WU Wen-hua, DU Ping-an, CHEN Yan, et al. The Application of large eddy simulation in aerodynamic noise simulation for axial fan [J]. Machine Design and Manufacture, 2013(1) : 63 – 65.
- [4] Jiménez Alvaro, Ángel y Crespo Martínez, Antonio y Migoya Valor, et al. Large-eddy simulation of spectral coherence in a wind turbine wake [J]. Environmental Research Letters, 2008, 3(1):1–9.
- [5] 刘秋洪,祁大同,曹淑珍.风机降噪研究的现状与分析 [J].流体机械,2001,29(2):29–33.
LIU Qiu-hong, QI Da-tong, CAO Shu-zhen. Review of research on fan noise reduction [J]. Fluid Machinery, 2001, 29(2) : 29 – 33.
- [6] 徐俊伟,吴亚锋,陈 耿.气动噪声数值计算方法的比较与应用 [J].噪声与振动控制,2012(4):6–9.
XU Jun-wei, WU Ya-feng, CHEN Geng. Comparison and application on the aero-acoustics numerical computing methods [J]. Noise and Vibration Control, 2012, 4: 6 – 9.
- [7] LARCHEVÈQUE L , SAGAUT P, MARY I. Large-eddy simulation of a compressible flow past a deep cavity [J]. Physics of Fluids, 2003, 15(1) : 193 – 211.
- [8] LENORMAND E, SAGAUT P. Subgrid-scale models for large-eddy simulations of compressible wall bounded flows [J]. AIAA Journal, 2000, 38(8) : 1340 – 1350.

(丛 敏 编辑)

cooling effect of turbine blade mid-chord. Cooling heat-transfer and flow resistance characteristics are obtained under various cooling flow rate in combined cooling structure of different spacing between impingement holes and film holes l/d_1 , the length of impingement hole h/d_1 . Meanwhile, the correlation is set up on cooling effect and structural feature parameter. The results show that in the structure of $l/d_1 = 12$, the cooling effectiveness outside surface of the film cooling holes both upstream and downstream is higher; and in the structure of $h/d_1 = 1$, the heat transfer coefficient on target surface increases. The cooling effectiveness outside surface of film cooling holes downstream is not affected by l and h. **Key words:** combined impingement-film cooling, cooling effectiveness, correlation

基于 Easy5 的燃气轮机发电系统建模与仿真 = **Modeling and Simulation of the Gas Turbine Power Generation System Based on Easy5** [刊, 汉] MEI Jiao-jiao, CHEN Jin-wei, ZHANG Hui-sheng, SU Ming(Gas Turbine Research Institute, Shanghai Jiaotong University, Shanghai, China, Post Code: 200240) //Journal of Engineering for Thermal Energy & Power. -2015, 30(4). -541 -546

With the modular modeling theory, a third-order synchronous generator module was established on a basis of the traditional nonlinear mathematical model of gas turbines. Based on the mathematical model, a complete model of single shaft gas turbine power generation system was built on Easy5 simulation platform. The variable load process of the entire gas turbine power generation system was simulated dynamically, which reflected the dynamic process of the gas turbine and generator well. Results agree well with the actual circumstances and the model has high versatility. **Key words:** modular modeling, gas turbine, generator, Easy5 simulation platform

低叶尖马赫数开式叶轮气动声源数值研究 = **Numerical Study on Aerodynamic Sound Sources of Low Tip Mach Number Open Impeller** [刊, 汉] WAN Jian-feng (School of Energy and Power Engineering, University of Shanghai for Science and Technology, Shanghai, China, Post Code: 200093) //Journal of Engineering for Thermal Energy & Power. -2015, 30(4). -547 -550

In order to find reasonable noise reduction measures, this paper, using Large Eddy Simulation and FW-H hybrid method, conducts a ful-scale simulation on flow and aerodynamic noise of low tip Mach open impeller and researches the aerodynamic sound sources performance. The study on SPL distribution in space and frequency domain shows: noise sources of the open impeller include monopole sound source, dipole sound source from blades rotation, and quadruple sound source generated by blade trailing vortex. There is not basically vortex-blade interference

noise in the open impeller. The quadruple sound source in the blade trailing is dissipated quickly, and can not able to be transferred to the downstream. The quadruple sound is not found in the open impeller downstream region. The main part of the open impeller noise is monopole noise, an important part of that is dipole noise, which is mainly concentrated in the tip region of the leading edge and the trailing edge. Sound Pressure (SP) of leading edge is greater than SP of trailing edge and SP of suction surface is greater than SP of pressure surface. **Key words:** open impeller, aerodynamic noise, Large Eddy Simulation, FW-H equation

基于高级过程仿真软件 APROS 的燃气轮机性能分析 = **Analysis of Gas Turbine Performance Based on the Advanced Process Simulation Software** [刊, 汉] ZHU Zheng-xiang, HAN Chao-bing, SI Feng-qi, (Key Laboratory of Energy Thermal Conversion and Control of Ministry of Education, Southeast University, Nanjing, China, Post Code: 210096), HUANG Zhi-jun (Datang Suzhou Thermal Power Co. Ltd., Wujiang, China, Post Code: 215214) //Journal of Engineering for Thermal Energy & Power. - 2015, 30(4). - 551 – 557

This paper gives a complete introduction of the simulation model of gas turbine and through comparing the simulation results with steady-state data on the spot, the accuracy of the simulation model is verified. Taking the PG9171E gas turbine as the object of study, the effect of the environment conditions on gas turbine performance was studied in this paper. Results indicate that the environment temperature has the biggest effect on the working characteristic and economy of the gas turbine. In the standard operating conditions, the heat consumption of gas turbine will increase by 0.2% with the ambient temperature rising one degree centigrade. In addition, the influence of air humidity will increase with the rising of temperature. When the environment temperature rises to 40 degrees, as the humidity increasing by each 10%, the heat consumption of gas turbine will increase by 0.12%. **Key words:** APROS, gas turbine, simulation model, ambient conditions

催化-预混混合燃烧室反应特性分析 = **A Study of Catalytic-premixed Hybrid Combustor Reaction Performance** [刊, 汉] WANG Yue (Faculty of Petroleum & Nature Gas Engineering, Liaoning Shihua University, Liaoning Fushun, China, Post Code: 113001), LIU Ai-guo (Faculty of Aerospace Engineering, Shenyang Aerospace University, Liaoning Shenyang, China, Post Code: 110136) //Journal of Engineering for Thermal Energy & Power. - 2015, 30(4). - 558 – 563

The structure of catalytic-premixed hybrid combustor has been mentioned which combines the catalytic combustion